TRANSPORT
ISSN 1648-4142 / eISSN 1648-3480
2022 Volume 37 Issue 6: 398–410
https://doi.org/10.3846/transport.2022.18172

REAR-END COLLISION ESCAPE ALGORITHM FOR INTELLIGENT VEHICLES SUPPORTED BY VEHICULAR COMMUNICATION

Chentong BIAN, Guodong YIN*, Liwei XU, Ning ZHANG

School of Mechanical Engineering, Southeast University, Nanjing, China

Submitted 7 January 2018, resubmitted 20 July 2018; accepted 13 September 2018

Abstract. To reduce rear-end collision risks and improve traffic safety, a novel rear-end collision escape algorithm is proposed for intelligent vehicles supported by vehicular communication. Numerous research has been carried out on rear-end collision avoidance. Most of these studies focused on maintaining a safe front clearance of a vehicle while only few considered the vehicle's rear clearance. However, an intelligent vehicle may be collided by a following vehicle due to wrong manoeuvres of an unskilled driver of the following vehicle. Hence, it is essential for an intelligent vehicle to maintain a safe rear clearance when there is potential for a rear-end collision caused by a following vehicle. In this study, a rear-end collision escape algorithm is proposed to prevent rear-end collisions by a following vehicle considering both straight and curved roads. A trajectory planning method is designed according to the motions of the considered intelligent vehicle and the corresponding adjacent vehicles. The successive linearization and the Model Predictive Control (MPC) algorithms are used to design a motion controller in the proposed algorithm. Simulations were performed to demonstrate the effectiveness of the proposed algorithm. The results show that the proposed algorithm is effective in preventing rear-end collisions caused by a following vehicle.

Keywords: rear-end collision, collision avoidance, model predictive control, intelligent vehicle, traffic safety, vehicular communication.

Introduction

With the growing number of vehicles, a very large number of traffic accidents occurs around the world; most of them caused by human factors. An effective way to prevent these traffic accidents is the application of intelligent vehicle technologies. Recently, several advanced technologies for intelligent vehicles (Eskandarian 2012) have been investigated to enhance vehicle performance and improve traffic safety. The rear-end collision avoidance system (Nekovee, Bie 2013) is one of the most popular study topics of intelligent vehicles. A variety of mass-produced passenger vehicles have been equipped with Autonomous Emergency Braking (AEB) systems to avoid rear-end collision. According to the road accident statistics in France (Fildes 2012), AEBs could reduce about 1.4% of fatal accidents and 4% of serious injuries each year. Specifically, a study indicated that the *Volvo XC60* with an AEB could have more than 20% fewer rear-end crashes (Rizzi *et al.* 2014). Using logistic regression, Fildes *et al.* (2015) analysed the rear-end traffic accident data in 6 countries and found that there is about 38% overall reduction of rear-end collision for the vehicles equipped with AEBs at low speeds. These analyses indicated that the previously investigated AEB is essential for the vehicles in order to reduce on-road rear-end collision accidents.

A variety of studies have been made for rear-end collision avoidance. These studies can be classified into 3 groups:

»» *the 1st group* focuses on rear-end collision warning systems. Based on vehicular ad-hoc networks and real-time traffic data, Lv *et al.* (2016) proposed a collision warning system to avoid rear-end collisions. When a potential rear-end collision is observed, the proposed system can transmit warning messages to drivers. Petrovai *et al.* (2016) designed a rear-end collision warning system based on stereovision, which is used to estimate the motion of the vehicle in front of a host vehicle. The system will issue a warning to the driver of the host vehicle when there is an imminent crash. Meng *et al.* (2015) introduced a method based on a dynamic vibrotactile collision

*Corresponding author. E-mail: *ygd@seu.edu.cn*

warning signal to warn drivers in dangerous conditions. The experiment results show that this method can significantly reduce the reaction times of drivers. Li *et al.* (2014) suggested a system for rear-end collision avoidance based on Vehicle-to-Vehicle (V2V) communication. When a vehicle is in danger of collision, the system will warn the driver of the vehicle to slow down. Using low cost inter-vehicular communications, Benedetto *et al.* (2015) investigated a collision warning system for preventing rear-end collisions. Yang *et al.* (2003) proposed an alerting system to prevent rear-end collision based on performance metrics;

»» *the 2nd group* focused on active speed control of vehicles. Kavitha *et al.* (2009) designed a rear-end collision avoidance system based on inter vehicle communication. Using the system, several vehicles can be slowed down when an emergency warning message is observed through V2V communication. Chen *et al.* (2016) proposed a rear-end collision avoidance system using a fuzzy logic controller. By the investigated controller, the relative distance can be maintained by the control of following vehicles. Kim *et al.* (2007) constructed a hierarchical layered structure to prevent rear-end collisions, where an upper layer was designed for the decision making of vehicle behaviour and a lower layer was constructed by the terminal sliding model method to control the longitudinal motion of the vehicle;

»» *the 3rd group* focused on combining braking and steering. Shah *et al.* (2015) proposed an integrated braking and steering control algorithm for rear-end avoidance, which can reduce traffic accidents by active lane changing. These studies are effective for reducing the risks of rear-end collisions and improving traffic safety, which are of great value for practical application.

While, most previous investigations on rear-end collision avoidance only considered the front clearances of host vehicles. The rear clearances were seldom discussed in these studies. Because of cost and personal preference, there are still many vehicles that are controlled by humans without any assistance system. Rear-end collisions will probably occur due to wrong manoeuvres of inexperienced drivers. Thus, an intelligent vehicle may be collided by a following vehicle driven by an unskilled driver. It is critical to design a control system for intelligent vehicles to prevent rear-end collisions caused by a following vehicle. However, few previous studies considered such a dangerous condition.

In this study, a rear-end collision escape algorithm is proposed for intelligent vehicles supported by vehicular communication. Different from conventional rear-end collision avoidance systems, which are design to maintain a safe front clearance, the proposed algorithm is investigated to maintain a safe rear clearance of an intelligent vehicle. To distinguish the objectives between the proposed algorithm and previous studies, the concept of rear-end collision escape is used to emphasize that the studied rear-end collision is caused by a vehicle, which is behind the host vehicle. Furthermore, the performance of lane keeping is considered in the proposed algorithm. Thus, the proposed algorithm can be used on general straight and curved roads.

The structure of the proposed algorithm is shown in Figure 1. There are 2 layers in the proposed algorithm:

»» *the upper layer* is the trajectory planning layer, which is designed to detect a potential rear-end collision and plan suitable trajectories. In this layer, a state machine is used to determine the planned trajectories. When there is no potential rear-end collision, the vehicle is in the normal state. When there is a potential rear-end collision, the vehicle turns to the escape state. The vehicle trajectory is planned according to the vehicle state. For the normal state, a cruise trajectory is planned for normal driving conditions when there is no frontal vehicle; a following trajectory is planned when there are frontal vehicles. For the escape state, an escape trajectory is planned for the host vehicle to avoid potential rear-end collisions; frontal trajectories will be planned for the frontal vehicles. The planned frontal trajectories can be sent to the corresponding vehicles by vehicular communication;

»» *the lower layer* is the motion controller layer including 2 controllers, which is investigated to track the planned trajectory. At any instance the considered intelligent vehicle is either in the normal state or in the escape state. Thus, there is only one kind of trajectory planned for the intelligent vehicle and one motion controller is used to control the vehicle.

The main contribution of this study is the proposal of a rear-end collision escape algorithm, which can maintain a safe rear clearance when there is a potential rear-end collision caused by a vehicle behind the host vehicle. The proposed algorithm can be applied for intelligent vehicles to prevent rear-end collisions and improve traffic safety.

The remainders of this paper are organized as following:

»» in Section 1, the problem of the considered rear-end collision escape is shown;

»» in Section 2, the method of trajectory planning is introduced;

»» in Section 3, vehicle models for the design of motion controllers are constructed;

»» in Section 4, motion controllers are designed for the considered intelligent vehicle to track the planned trajectory;

»» in section 5, simulations on different roads are conducted to verify the effectiveness of the proposed algorithm;

»» finally, the conclusions of this paper are made as a summary.

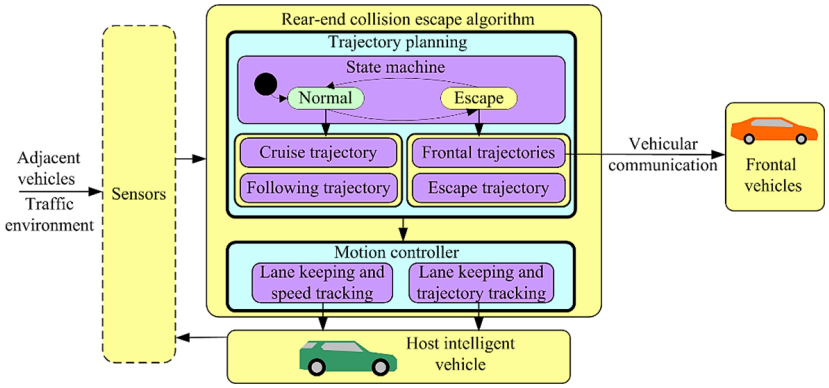

Figure 1. Structure of a rear-end collision escape algorithm (source: created by the authors)

1. Problem statement

The problem of the considered rear-end collision escape is shown in Figure 2, in which there is an intelligent vehicle (host vehicle), a following vehicle and n frontal vehicles. One possible condition is $n = 0$, which means that there is only a following vehicle and an intelligent vehicle (host vehicle). The intelligent vehicle and frontal vehicles are equipped with vehicular communication devices. Under a dangerous condition, the host vehicle can send planned trajectories to the frontal vehicles and the frontal vehicles can follow the planned trajectories. Without considering rear-end collisions from the back of the host vehicle, this vehicle should follow a desired speed when $n = 0$ or follow the adjacent frontal vehicle when $n \geq 1$, respectively. Obviously, a rear-end collision will occur if the following vehicle moves with high speed towards the intelligent vehicle, which may be caused by wrong manoeuvres of an unskilled driver of the following vehicle. There are 3 objectives that should be achieved for the proposed algorithm:

- the considered rear-end collision should be avoided;
- the frontal clearance of the host vehicle should be maintained if there are frontal vehicles;
- the intelligent vehicle should follow the road path without departure.

The path and the motion sates of the considered vehicles can be obtained by product sensors and vehicular communication, which are not the focus of this study. The investigated intelligent vehicle is equipped with 4 in-wheel motors, which can directly control the drive torque of each wheel.

For a road with multiple lanes, rear-end collisions can be easily avoided by the manoeuvre of lane changing. However, it is much more dangerous for rear-end collisions on a single-lane road, because a lane changing manoeuvre cannot be conducted in this situation. Hence, in this study, a single-lane road is considered.

2. Trajectory planning algorithm

The key point of rear-end collision escape is to maintain a safe rear clearance of an intelligent vehicle. When there is a potential rear-end collision, the intelligent vehicle should speed up and maintain a safe clearance from the following vehicle. If there are frontal vehicles ahead of the intelligent vehicle, the intelligent vehicle should plan safe trajectories for the frontal vehicles and send the trajectories to the frontal vehicles. Following the planned trajectories, the frontal vehicles can also speed up and maintain a safe clearance with the intelligent vehicle. When there is no potential rear-end collisions, the intelligent vehicle should follow the desired speed or the adjacent frontal vehicles. In this section, 4 kinds of trajectories are designed for rear-end collision escape and normal driving.

2.1. Car-following model

Before the discussion of trajectory planning, a car-following model is discussed to analyse the considered rear-end problem. A variety of car-following models have been proposed in previous studies. Hoogendoorn *et al.* (2010) compared the Helly's model and intelligent driver model using a driving simulator and found that the Helly's model is more suitable for experimental data. Based on optical information, Andersen and Sauer (2007) proposed a Driving by Visual Angle (DVA) model for car-following control. Instead of the relative speed and clearance to the frontal vehicle, the visual information is used for the DVA model to determine the controlled acceleration. Rakha *et al.* (2009) designed a simplified car-following model that took traffic stream parameters into account. Considering the influence of space gap, Li *et al.* (2018) investigated a car-following model that focused on the response of drivers to velocity difference. Among these models, the Helly's driver model is of a simple structure and can be easily applied in analysis and simulation. Moreover, this

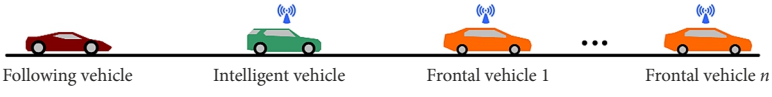

Figure 2. Problem of rear-end collision escape (source: created by the authors)

model is also found to be suitable for the study of driver behaviour in fog weather (Hoogendoorn *et al.* 2010). Thus, in this study, the Helly's driver model is considered:

$$a(t) = \alpha \cdot \Delta v \cdot (t - \tau) + \beta \cdot (c \cdot (t - \tau) - S), \quad (1)$$

where: a is the controlled longitudinal acceleration of the driver; α, β are the parameters of the driver model; τ is the reaction delay time; Δv means the difference between the frontal speed and the vehicle speed; c is the actual clearance between vehicles; S is the desired clearance with the frontal vehicle; t is time.

Equation (1) indicates that, under normal conditions, the driver can maintain a synchronous speed and a safe clearance with the frontal vehicle.

2.2. Assertion of potential rear-end collision

Under dangerous conditions, such as fog and attention diversion, a driver may fail to maintain sufficient clearance and collide with the frontal vehicle. A commonly used index to measure such a dangerous condition is Time To Collision (TTC) (Li *et al.* 2016). If TTC is too low, it is reasonable to deduce that there is potential for a rear-end collision accident. Therefore, if the control system of the host vehicle detects that the TTC between it and the following vehicle is to low, the host vehicle should speed up to avoid a potential rear-end collision. In this study, a TTC threshold is used to assert the potential for a rear-end collision:

$$t_c < t_{cri}, \quad (2)$$

where: t_{cri} is the threshold for a potential accident, which is a commonly used method to assert rear-end collisions; t_c is TTC.

On the one hand, if the actual TTC is higher than t_{cri}, the algorithm will assume the driver of the following vehicle can maintain a safe clearance. On the other hand, if the actual clearance is lower than t_{cri}, the algorithm will assume that the driver of the following vehicle may cause a rear-end collision accident.

2.3. State machine

When there is a potential rear-end collision, the rear clearance should be considered for the intelligent vehicle. When there is no potential rear-end collision, the intelligent vehicle should follow the desired speed or the frontal adjacent vehicle. Thus, the trajectory of the intelligent vehicle should be planned based on different conditions of the vehicle.

As shown in Figure 3, a state machine, which includes a normal state and an escape state, is designed for the intelligent vehicle. If the TTC between the following vehicle and the host vehicle is lower than the threshold, it can be deduced that the driver of the following vehicle may fail to maintain a safe clearance. A rear-end collision will probably occur without proper control of the intelligent vehicle. Hence, the intelligent vehicle should turn to the escape state under that condition and the manoeuvre of rear-end collision escape should be conducted. There are

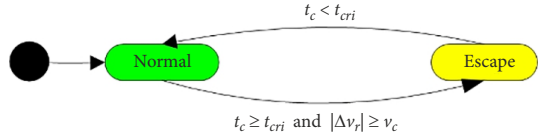

Figure 3. State machine (source: created by the authors)

2 conditions that should be satisfied if the state changes to a normal state:

- the 1st one is $t_c \geq t_{cri}$, which means a sufficient TTC;
- the 2nd one is $|\Delta v_r| \geq v_c$, where Δv_r is the change of the speed of the following vehicle and v_c is a constant threshold.

This condition is used to ensure that the driver of the following vehicle can control the speed of the following vehicle. If there is attention diversion of the driver and the driver fails to adjust the speed, the intelligent vehicle should escape and maintain a sufficient clearance from the following vehicle.

2.4. Trajectory design

As there are 2 states of the intelligent vehicle, considering the presence of frontal vehicles, 4 kinds of trajectories are designed. Since a single-lane road, path planning is not considered in this study. The intelligent vehicle should follow the lane on the road.

2.4.1. Trajectory planning in the normal state

When the vehicle is in the normal state, if there are no frontal vehicles, the planned cruise trajectory for the host vehicle can be expressed as:

$$v_p = v_{nd}, \quad (3)$$

where: v_p is planned speed of the intelligent vehicle; v_{nd} is desired speed of the intelligent vehicle.

Equation (3) means that there is no constraint of the longitudinal position of the intelligent vehicle. It is desirable for the intelligent vehicle to follow the desired speed along the path.

If there are frontal vehicles, the intelligent vehicle should maintain synchronous speed and safe clearance from the adjacent frontal vehicle. The following trajectory is planned for the host vehicle to satisfy such requirements:

$$\begin{cases} s_p = s_f - d_s; \\ v_p = v_f, \end{cases} \quad (4)$$

where: s_p means the planned longitudinal position of the intelligent vehicle along the path; v_p is planned speed of the intelligent vehicle; s_f is longitudinal position of the adjacent frontal vehicle; v_f is the longitudinal speed of the adjacent frontal vehicle; d_s is the desired clearance, which can be expressed as:

$$d_s = s_0 + h_{\min} \cdot v_f, \quad (5)$$

where: s_0, $h_{\min}$ are parameters for determining the desired clearance.

2.4.2. Trajectory planning in escape state

When the vehicle is in the escape state, to avoid rear-end collision with the following vehicle, the planned escape trajectory of the host vehicle can be expressed as:

$$\begin{cases} s_p = s_r + d_r; \\ v_p = v_r, \end{cases} \tag{6}$$

where: s_r means the longitudinal position of the following vehicle along the path; v_r is speed of the following vehicle; d_r is the desired rear clearance, which is calculated as:

$$d_r = \min\left(d_s, f_g \cdot d_g\right), \tag{7}$$

where: d_g is the visible distance in fog weather; f_g is a factor to calculate the rear clearance ($f_g < 1$).

Generally, in fog weather, it is more suitable to maintain the frontal vehicle within a visible distance (Wu *et al.* 2017). The above equation means that, if there is fog weather, the intelligent vehicle should be within the sight of the driver of the following vehicle. Thus, the driver can see the intelligent vehicle and follow the intelligent vehicle safely. Otherwise, the driver cannot see the intelligent vehicle and might maintain an unsafely high speed.

Equation (6) means the intelligent vehicle should maintain a synchronous speed and safe clearance from the following vehicle. However, if the speed of the intelligent vehicle is too high, the vehicle may collide with the frontal vehicle. To handle this problem, the intelligent vehicle should plan safe trajectories for the frontal vehicles. Following the planned trajectories, the frontal vehicles can maintain a safe clearance with the intelligent vehicle. Based on the discussion above, the frontal trajectories can be planned for the frontal vehicles as:

$$\begin{cases} s_{p,f,i} = s_r + d_r + d_s \cdot i; \\ v_{p,f,i} = v_r, \end{cases} \tag{8}$$

where: $s_{p,\,f,\,i}$ is planned longitudinal position of the ith frontal vehicle; $p_{p,\,f,\,i}$ is planned longitudinal speed of the ith frontal vehicle.

The Equation (8) means that, similar to the intelligent vehicle, the frontal vehicles should also maintain a synchronous speed with the following vehicle. The clearances between the intelligent vehicle and the frontal vehicles are d_s. Following the planned trajectories, the frontal vehicles will not collide with the intelligent vehicle.

3. Vehicle modelling

In this section, several vehicle models are constructed for the design of motion controllers:

- »» the longitudinal and lateral dynamic model of the intelligent vehicle is constructed;
- »» the model of path tracking is built;
- »» then, the model of trajectory tracking is shown;
- »» at last the model of path tracking and speed tracking is provided.

The constructed models provide a foundation of the motion controller design.

3.1. Longitudinal and lateral dynamic model

As shown in Figure 4, a single-track model considering the planar motion with 3 degree-of-freedom is employed. It is assumed that the vehicle is moving on a horizontal level road without wind. The longitudinal and lateral dynamics vehicle model can be written as (Yin *et al.* 2011):

$$\begin{cases} \dot{v}_x = v_y \cdot \omega_r + a_1 \cdot v_x^2 + b_1 \cdot F_x; \\ \dot{v}_y = a_2 \cdot \dfrac{v_y}{v_x} + \left(\dfrac{a_3}{v_x} - v_x\right) \cdot \omega_r + b_2 \cdot \delta; \\ \dot{\omega}_r = a_4 \cdot \dfrac{v_y}{v_x} + a_5 \cdot \dfrac{\omega_r}{v_x} + b_3 \cdot \delta + b_4 \cdot M_\Delta, \end{cases} \tag{9}$$

where:

$$a_1 = -\frac{1}{2 \cdot m} \cdot C_D \cdot A_R \cdot \rho;$$

$$a_2 = -\frac{C_f + C_r}{m};$$

$$a_3 = -\frac{C_f \cdot l_f - C_r \cdot l_r}{m};$$

$$a_4 = -\frac{l_f \cdot C_f - l_r \cdot C_r}{I_z};$$

$$a_5 = -\frac{l_f^2 \cdot C_f + l_r^2 \cdot C_r}{I_z};$$

$$b_1 = \frac{1}{m};$$

$$b_2 = \frac{C_f}{m};$$

$$b_3 = \frac{l_f \cdot C_f}{I_z};$$

$$b_4 = \frac{1}{I_z};$$

ω_r denotes the yaw rate; v_x, v_y are the longitudinal and lateral velocities at the Centre of Gravity (CoG) of the vehicle, respectively; m is the total mass; I_z is the moment of inertia round the vertical axis; C_f, C_r are the front and rear axle cornering stiffness, respectively; C_D represents the air drag coefficient factor; A_r denotes the vehicle front area; ρ is the air density; because the lateral velocity is

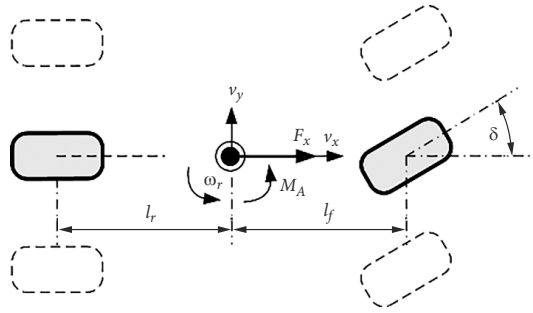

Figure 4. Single-track model (source: created by the authors)

small, only the longitudinal air drag force is taken into consideration; the dynamics of the wheel and motor are ignored; δ is the steering angle; F_x represents the resultant force of the longitudinal tire forces with respect to the longitudinal direction $\left(F_x = \left(T_{lf} + T_{fr} + T_{rl} + T_{rr}\right)\right)$; R_w represents the resultant force of the longitudinal tire forces with respect to the longitudinal direction; T_i when i = *fl*, *fr*, *rl*, *rr* represents the drive torque of the front-left, front-right, rear-left and rear-right wheels, respectively; M_Δ is the resultant yaw moment of the longitudinal tire forces $\left(M_\Delta = l_s \cdot R_w \cdot \left(T_{fr} + T_{rr} - T_{fl} - T_{rl}\right)\right)$; l_s is half of the wheel tread; R_w is the radius of each wheel.

Note that, in Equation (9), the control inputs are defined as δ, F_x and M_Δ, which should be calculated from the motion controller. After obtaining these control inputs, the drive torque of each wheel can be calculated as:

$$\begin{cases} T_{fl} = \left(F_x - \dfrac{M_\Delta}{2 \cdot l_s}\right) \cdot R_w; \\ T_{rl} = \left(F_x - \dfrac{M_\Delta}{2 \cdot l_s}\right) \cdot R_w; \\ T_{fr} = \left(F_x + \dfrac{M_\Delta}{2 \cdot l_s}\right) \cdot R_w; \\ T_{rr} = \left(F_x + \dfrac{M_\Delta}{2 \cdot l_s}\right) \cdot R_w. \end{cases} \tag{10}$$

3.2. Path tracking model

The trajectory tracking model of the intelligent vehicle is shown in Figure 5, which is used to demonstrate the relative motion of the intelligent vehicle to a path. There are 3 key points in this figure:

- »» point p_d is the desired point at that time;
- »» point CoG is the CoG of the vehicle;
- »» point p_c is the closest point on the path to point CoG.

The position error along the path is e_1, the distance between p_c and CoG is e_2 and the yaw angle error is e_3. Assuming e_3 is small, one has:

$$\begin{cases} \dot{e}_1 = -v_y \cdot e_3 + v_x - v_p; \\ \dot{e}_2 = v_y + v_x \cdot e_3; \\ \dot{e}_3 = \omega_r - \omega_{des}, \end{cases} \tag{11}$$

where: $\omega_{des} = \dfrac{v_p}{R}$ is the desired yaw rate; R is the path radius at p_c.

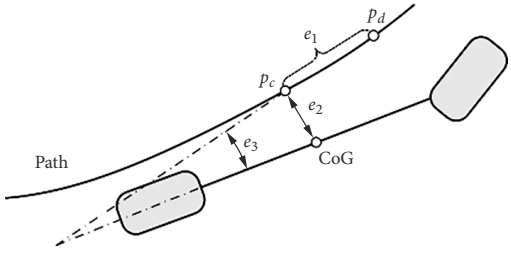

Figure 5. Path tracking model (source: created by the authors)

As to the trajectory tracking performance, the desired longitudinal, lateral position errors and yaw angle error are defined as $e_{1d} = 0$, $e_{2d} = 0$ and $e_{3d} = 0$, respectively.

3.3. Trajectory tracking model

When the intelligent vehicle is in the escape state or following the frontal vehicle, it is desirable to track the planned trajectory along the desired path and longitudinal position. Since the trajectories shown in Equations (4) and (6) define a moving point along the path, Equation (11) can describe the error of the vehicle to the planned trajectory. Combining Equations (9) and (11), the trajectory tracking model of the escape state can be expressed as:

$$\begin{cases} \dot{e}_1 = -v_y \cdot e_3 + v_x - v_p; \\ \dot{e}_2 = v_y + v_x \cdot e_3; \\ \dot{e}_3 = \omega_r - \omega_{des}; \\ \dot{v}_x = v_y \cdot \omega_r + a_1 \cdot v_x^2 + b_1 \cdot F_x; \\ \dot{v}_y = a_2 \cdot \dfrac{v_y}{v_x} + \left(\dfrac{a_3}{v_x} - v_x\right) \cdot \omega_r + b_2 \cdot \delta; \\ \dot{\omega}_r = a_4 \cdot \dfrac{v_y}{v_x} + a_5 \cdot \dfrac{\omega_r}{v_x} + b_3 \cdot \delta + b_4 \cdot M_\Delta. \end{cases} \tag{12}$$

3.4. Path tracking and speed tracking model

When the intelligent vehicle is in the normal state without frontal vehicles, it is desirable to track the planned speed and follow the path for the intelligent vehicle. Compared with Equation (6), there is no constraint for the longitudinal position of the intelligent vehicle in the trajectory defined in Equation (3). Thus, e_1 is ignored. According to Equations (9) and (11), the path tracking and speed tracking model can be expressed as:

$$\begin{cases} \dot{e}_2 = v_y + v_x \cdot e_3; \\ \dot{e}_3 = \omega_r - \omega_{des}; \\ \dot{v}_x = v_y \cdot \omega_r + a_1 \cdot v_x^2 + b_1 \cdot F_x; \\ \dot{v}_y = a_2 \cdot \dfrac{v_y}{v_x} + \left(\dfrac{a_3}{v_x} - v_x\right) \cdot \omega_r + b_2 \cdot \delta; \\ \dot{\omega}_r = a_4 \cdot \dfrac{v_y}{v_x} + a_5 \cdot \dfrac{\omega_r}{v_x} + b_3 \cdot \delta + b_4 \cdot M_\Delta. \end{cases} \tag{13}$$

4. Controller design

The models shown in Equations (12) and (13) are nonlinear, which are hard to analyse using conventional linear control algorithms. Thus, the successive linearization (Zhai *et al.* 2010) is utilized for these models. At each sample time, the constructed models are linearized at current states. Then the linearized models are discretized to facilitate the application of Model Predictive Control (MPC) (Camacho, Bordons 2007). In the previous section, there were 3 kinds of trajectories designed for the intelligent vehicle. In this section, a trajectory tracking controller is designed to track the following trajectory and the escape trajectory; a path tracking and speed tracking controller is designed to track the cruise trajectory.

4.1. Linearization and discretization for the model of trajectory tracking

According to the 1st order linearization (Zhai *et al.* 2010), the model represented by Equation (12) can be approximated by:

$$\begin{cases} \dot{e}_1 = -v_{y0}e_3 - e_{30}v_y + v_{y0}e_{30} + v_x - v_p; \\ \dot{e}_2 = v_{x0}e_3 + e_{30}v_x + v_y - v_{x0}e_{30}; \\ \dot{e}_3 = \omega_r - \omega_{des}; \\ \dot{v}_x = eqs_1; \\ \dot{v}_y = eqs_2; \\ \dot{\omega}_r = eqs_3, \end{cases} \tag{14}$$

where:

$$eqs_1 = 2 \cdot a_1 \cdot v_{x0} \cdot v_x + \omega_{r0} \cdot v_y + v_{y0} \cdot \omega_r - \omega_{r0} \cdot v_{y0} - 2 \cdot a_1 \cdot v_{x0}^2 + b_1 \cdot F_{x0} + b_1 \cdot F_x;$$

$$eqs_2 = \left(-a_2 \cdot \frac{v_{y0}}{v_{x0}^2} - a_3 \cdot \frac{\omega_{r0}}{v_{x0}^2} - \omega_{r0} \right) \cdot v_x + a_2 \cdot \frac{1}{v_{x0}} \cdot v_y + \left(a_3 \cdot \frac{1}{v_{x0}} - v_{x0} \right) \cdot \omega_r + a_2 \cdot \frac{v_{y0}}{v_{x0}} + a_3 \cdot \frac{\omega_{r0}}{v_{x0}} + \omega_{r0} \cdot v_{x0} + b_2 \cdot \delta_0 + b_2 \cdot \delta;$$

$$eqs_3 = \left(-a_4 \cdot \frac{v_{y0}}{v_{x0}^2} - a_5 \cdot \frac{\omega_{r0}}{v_{x0}^2} \right) \cdot v_x + a_4 \cdot \frac{1}{v_{x0}} \cdot v_y + a_5 \cdot \frac{1}{v_{x0}} \cdot \omega_r + a_4 \cdot \frac{v_{y0}}{v_{x0}} + a_5 \cdot \frac{\omega_{r0}}{v_{x0}} + b_3 \cdot \delta_0 + b_4 \cdot M_{\Delta 0} + b_3 \cdot \delta + b_4 \cdot M_{\Delta},$$

where: v_{x0}, v_{y0}, ω_{r0}, e_{30} are current states; F_{x0}, δ_0, $M_{\Delta 0}$ are the previous control inputs.

Equation (14) can be rewritten as:

$$\dot{\mathbf{x}}_c = \mathbf{A}_c \cdot \mathbf{x}_c + \mathbf{B}_c \cdot \mathbf{u}_c + \mathbf{E}_c \cdot \mathbf{d}_c, \tag{15}$$

where: $\mathbf{E}_c$ is an identity matrix;

$$\mathbf{x}_c = \begin{bmatrix} e_1 \\ e_2 \\ e_3 \\ v_x \\ v_y \\ \omega_r \end{bmatrix};$$

$$\mathbf{u}_c = \begin{bmatrix} F_x \\ \delta \\ M_{\Delta} \end{bmatrix};$$

$$\mathbf{d}_c = \begin{bmatrix} d_1 \\ d_2 \\ d_3 \\ d_4 \\ B_1 \\ B_2 \end{bmatrix},$$

where:

$$d_1 = v_{y0} \cdot e_{20} - v_p;$$

$$d_2 = -v_{x0} \cdot e_{20};$$

$$d_3 = -\omega_{des};$$

$$d_4 = -\omega_{r0} \cdot v_{y0} - 2 \cdot a_1 \cdot v_{x0}^2 + b_1 \cdot F_{x0};$$

$$B_1 = a_2 \cdot \frac{v_{y0}}{v_{x0}} + a_3 \cdot \frac{\omega_{r0}}{v_{x0}} + \omega_{r0} \cdot v_{x0} + b_2 \cdot \delta_0;$$

$$B_2 = a_4 \cdot \frac{v_{y0}}{v_{x0}} + a_5 \cdot \frac{\omega_{r0}}{v_{x0}} + b_3 \cdot \delta_0 + b_4 \cdot M_{\Delta 0};$$

$$\mathbf{A}_c = \begin{bmatrix} 0 & 0 & -v_{y0} & 1 & -e_{30} & 0 \\ 0 & 0 & v_{x0} & e_{30} & 1 & 1 \\ 0 & 0 & 0 & 0 & 0 & 1 \\ 0 & 0 & 0 & A_7 & \omega_{r0} & v_{y0} \\ 0 & 0 & 0 & A_1 & A_2 & A_3 \\ 0 & 0 & 0 & A_4 & A_5 & A_6 \end{bmatrix},$$

where:

$$A_1 = -a_2 \cdot \frac{v_{y0}}{v_{x0}^2} - a_3 \cdot \frac{\omega_{r0}}{v_{x0}^2} - \omega_{r0};$$

$$A_2 = a_2 \cdot \frac{1}{v_{x0}};$$

$$A_3 = a_3 \cdot \frac{1}{v_{x0}} - v_{x0};$$

$$A_4 = -a_4 \cdot \frac{v_{y0}}{v_{x0}^2} - a_5 \cdot \frac{\omega_{r0}}{v_{x0}^2};$$

$$A_5 = a_4 \cdot \frac{1}{v_{x0}};$$

$$A_6 = a_5 \cdot \frac{1}{v_{x0}};$$

$$\mathbf{B}_c = \begin{bmatrix} 0 & 0 & 0 \\ 0 & 0 & 0 \\ 0 & 0 & 0 \\ b_1 & 0 & 0 \\ 0 & b_2 & 0 \\ 0 & b_3 & b_4 \end{bmatrix}.$$

The model in Equation (15) can be discretized by the conventional forward Euler scheme with a fixed sampling time T_s:

$$\mathbf{x}_{k+1} = \mathbf{A} \cdot \mathbf{x}_k + \mathbf{B} \cdot \mathbf{u}_k + \mathbf{E} \cdot \mathbf{d}_k, \tag{16}$$

where: k is the current time step; $\mathbf{x}_k$, $\mathbf{u}_k$, $\mathbf{d}_k$ are the discretized system states, control inputs and disturbances, respectively; $\mathbf{A}$, $\mathbf{B}$, $\mathbf{E}$ denote the matrices of the discretized system with respect to the corresponding continuous model in Equation (15).

4.2. Constraints of controller

The system inputs and speed should be limited to avoid exceeding physical limits. The constraints of the system inputs are written as:

$$\mathbf{u}_{\min} \le \mathbf{u}_k \le \mathbf{u}_{\max}, \tag{17}$$

where:

$$\mathbf{u}_{\min} = \begin{bmatrix} F_{x\min} & \delta_{\min} & M_{\Delta\min} \end{bmatrix}^T;$$

$$\mathbf{u}_{\max} = \begin{bmatrix} F_{x\max} & \delta_{\max} & M_{\Delta\max} \end{bmatrix}^T,$$

where: $\delta_{\min}$, $F_{x\min}$, $M_{\Delta\min}$ are the lower limits of the corresponding control inputs, respectively; $\delta_{\max}$, $F_{x\max}$, $M_{\Delta\max}$ are the upper limits of the corresponding control inputs, respectively.

The constraints of vehicle speed are written as:

$$v_{x\min} \le v_x \le v_{x\max}, \tag{18}$$

where: $v_{x\min}$ is the lower limit of the vehicle speed; $v_{x\max}$ is the upper limit of the vehicle speed.

4.3. Trajectory tracking controller

After obtaining the discretized model shown in Equation (16), the trajectory tracking controller can be designed based on the MPC. In the MPC algorithm, the future states of the controlled system can be predicted based on the current state and the control inputs within certain predictive horizons. Based on these predicted states, the performance of the controller can be optimized to calculate the optimal control input. At each sampling instance, only the 1st element of the control input is used, and the optimization is repeated at the next sampling instance (Camacho, Bordons 2007).

In the predictive model shown in Equation (15), there may exist model mismatch caused by parameters uncertainty, which can be handled using a feedback correction method (Deng 2000). In each control step, the predicted error can be estimated by comparing the predicted states in the previous step and the measured state in the current step:

$$\mathbf{e}_k = \mathbf{x}_{(k|k-1)} - \mathbf{x}_k, \tag{19}$$

where: $(k + i|k)$ means the predicted value at step $k + 1$ based on the information at step k.

To reduce the effects of parameter uncertainties, based on the feedback correction method (Deng 2000), the predictive model in Equation (16) can be rewritten as:

$$\mathbf{x}_{k+1} = \mathbf{A}\cdot\mathbf{x}_k + \mathbf{B}\cdot\mathbf{u}_k + \mathbf{E}\cdot\mathbf{d}_k + \boldsymbol{\varepsilon}_k, \tag{20}$$

where: $\boldsymbol{\varepsilon}_k = h\cdot\mathbf{e}_k$ is the feedback correction item, which is defined to compensate model uncertainty (where: h is a constant factor of the feedback correction).

At step k, the future control inputs can be represented by:

$$\mathbf{q}_k = \begin{bmatrix} \mathbf{u}_{(k|k)}^T & \mathbf{u}_{(k+1|k)}^T & \cdots & \mathbf{u}_{(k+c-1|k)}^T \end{bmatrix}^T, \tag{21}$$

where: $(k + i|k)$ means the predicted value at step $k + 1$ based on the information at step k; c is the control horizon ($c = 7$).

The future states of the system can be predicted using the iterative calculation of Equation (16):

$$\begin{cases} \mathbf{x}_{(k+1|k)} = \mathbf{A}\cdot\mathbf{x}_k + \mathbf{B}\cdot\mathbf{u}_{(k|k)} + \mathbf{E}\cdot\mathbf{d}_k + \boldsymbol{\varepsilon}_k; \\ \mathbf{x}_{(k+2|k)} = \mathbf{A}\cdot\mathbf{x}_{(k+1|k)} + \mathbf{B}\cdot\mathbf{u}_{(k+1|k)} + \mathbf{E}\cdot\mathbf{d}_{(k+1|k)} + \boldsymbol{\varepsilon}_{(k+1|k)}; \\ \vdots \\ \mathbf{x}_{(k+p-1|k)} = \mathbf{A}\cdot\mathbf{x}_{(k+p-2|k)} + \mathbf{B}\cdot\mathbf{u}_{(k+p-2|k)} + \mathbf{E}\cdot\mathbf{d}_{(k+p-2|k)} + \boldsymbol{\varepsilon}_{(k+p-2|k)}; \\ \mathbf{x}_{(k+p|k)} = \mathbf{A}\cdot\mathbf{x}_{(k+p-1|k)} + \mathbf{B}\cdot\mathbf{u}_{(k+p-1|k)} + \mathbf{E}\cdot\mathbf{d}_{(k+p-1|k)} + \boldsymbol{\varepsilon}_{(k+p-1|k)}, \end{cases} \tag{22}$$

where: p is the predicted horizon ($p = 7$).

Equation (22) indicates that the future system states can be predicted based on the planned control inputs. Thus, the optimal control performance can be obtained by optimizing the future control inputs. The aim of the controller is to track the planned trajectory. To achieve this task, the objective function L is defined as:

$$L(\mathbf{q}_k) = \sum_{i=0}^{c-1} \mathbf{w}_u \cdot \left(\mathbf{u}_{(k+i|k)}\right)^2 + \sum_{i=1}^{p} \mathbf{w}_x \cdot \left(\mathbf{r}_{(k+i|k)} - \mathbf{x}_{(k+i|k)}\right)^2 + \sum_{i=0}^{c-1} \mathbf{w}_{\Delta u} \cdot \left(\mathbf{u}_{(k+i|k)} - \mathbf{u}_{(k+i-1|k)}\right)^2, \tag{23}$$

where: $\mathbf{w}_u$, $\mathbf{w}_{\Delta u}$, $\mathbf{w}_x$ are the weight matrices of input, incensement of input and state error, respectively; $\mathbf{r}$ represents the desired value $\left(\mathbf{r} = \begin{bmatrix} e_{1d} & e_{2d} & e_{3d} & v_p & v_{yd} & \omega_{des} \end{bmatrix}^T\right)$.

A large lateral velocity may lead to instability; hence, it is preferred to keep the lateral velocity as low as possible. Thus $v_{yd} = 0$ is set as the desired value.

At each sampling instant, the future states can be predicted based on Equation (22). The optimization problem of the controller is solved as:

$$\min L(\mathbf{q}_k), \tag{24}$$

subjected to: Equations (17) and (18).

Using sophisticated optimal methods such as interior-point (Wächter, Biegler 2006) and active-set (Birgin, Mario Martínez 2002), the optimization problem can be solved. Then the steering angle, the resultant longitudinal force and the resultant yaw moment are obtained. The drive torque of each wheel can be calculated through Equation (10).

4.4. Path tracking and speed tracking controller

Similar to the design of the trajectory tracking controller, the path tracking and speed tracking controller can be designed based on the model shown in Equation (13) by the same method as the design of the trajectory tracking controller. Using 1st order linearization and a forward Euler scheme, a discretized model similar to Equation (16) can be obtained. The constraints of the system inputs and speed in Equations (17) and (18) can be used as well. Then an objective function can be constructed considering the discretized model and constraints. Finally, the optimization problem can be solved using sophisticated optimization methods and optimal control can be obtained to control the intelligent vehicle.

5. Numerical simulation

In this section, 3 simulations are conducted using MATLAB (*https://www.mathworks.com/products/matlab.html*) and CarSim (*https://www.carsim.com*) to show the effectiveness of the proposed algorithm. The driver model described in Equation (1) is used to control the following vehicle. Both straight and curved roads are considered in these simulations. The main parameters of the intelligent vehicle used in simulation are listed in Table. The complex collision analysis is not considered in the simulation. Thus, the effect of rear-end collisions on these vehicles are ignored to simplify the problem. If the clearance between 2 vehicles is lower than zero, a rear-end collision will occur. For simplification, in this section, the Following Vehicle is represented by FV; the Intelligent Vehicle is denoted by IV; the FRontal Vehicle is represented by FRV.

5.1. Simulation on a straight road with no frontal vehicle

In this simulation, a probabilistic approach including 2 groups of scenarios is constructed to evaluate the proposed method. Each group consists of 100 scenarios for comparison. In the 1st group, the escape algorithm is not considered for the intelligent vehicle. In the 2nd group, the escape algorithm is considered. The initial conditions between the scenarios among these groups are a one-on-one correspondence. The initial and desired speed of the intelligent vehicle is 20 m/s as plotted in Figure 6a. For each scenario, a straight road is used as indicated in Figure 6b. In these scenarios, the initial speeds and frontal clearances of the following vehicle, the visible distance, and the attention division times of the driver are randomly selected from the following range: the initial speeds of the following vehicle range from 21 to 25 m/s; the initial frontal clearances of the following vehicle range from 30 to 100 m; the visible distances range from 30 to 500 m; the attention division times of the driver range from 15 to 18 s. Due to the attention diversion of the driver of the following vehicle, the driver does not notice the intelligent vehicle at the beginning. The statistics of the simulation results are plotted in Figure 7.

As indicated in Figure 7a, without considering rear-end escape, there are totally 34 rear-end collisions among the 100 conducted scenarios, which indicates that it is critical to maintain a safe rear clearance for an intelligent vehicle. Since a following vehicle controlled by an unskilled driver may lead to dangerous accidents. The rear clearance of an intelligent vehicle should be considered to avoid the collision caused by a following vehicle. For the group with rear-end escape, no rear-end collision occurred among the considered scenarios. It can be found that the proposed algorithm can prevent a potential rear-end collision caused by the following vehicle. The main reason is that the proposed algorithm can maintain a certain rear clearance between the host vehicle and the following vehicle. Hence, when undesired potential rear-end collisions could occur,

Table. Vehicle parameters

Parameter	Value
m	1412 kg
I_z	1537.7 kg·m^2
l_f	1.016 m
$M_{\Delta\max}$	3000 N·m
$\delta_{\min}$	–10°
l_s	0.77 m
C_f	86304 N/rad
C_r	67574 N/rad
$M_{\Delta\min}$	–3000 N·m
$F_{x\max}$	3000 N
k_s	2 s
d_0	4 m
l_r	1.564 m
$\delta_{\max}$	10°
$F_{x\min}$	–3000 N

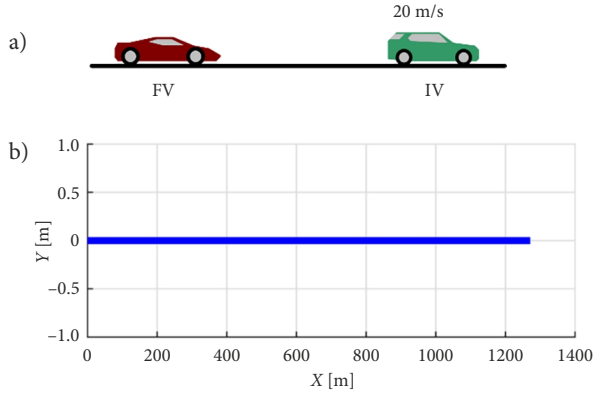

Figure 6. Path and initial condition (source: created by the authors): a – initial condition; b – path; FV – following vehicle; IV – intelligent vehicle

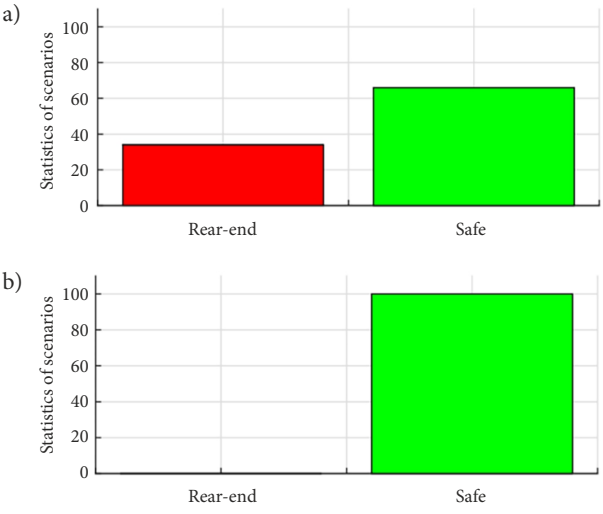

Figure 7. Statistics of the simulation scenarios (source: created by the authors): a – without rear-end escape; b – with rear-end escape

the host vehicle can speed up and maintain the rear clearance and avoid such collision accidents. This simulation demonstrates that, the proposed algorithm can guarantee the rear-end collision escape performance of the intelligent vehicle on a straight road.

5.2. Simulation on a clothoid road with a single frontal vehicle

In this simulation, a clothoid road with a decelerating frontal vehicle is considered. A frontal vehicle and a following vehicle of the host vehicle are considered. The following vehicle is controlled by a driver and the driver does not observe the intelligent vehicle in the beginning due to attention diversion. The initial longitudinal positions of the considered vehicles and the road path are plotted in Figure 8. Without the proposed algorithm, the speeds of these vehicles are shown in Figure 9a. The clearances among these vehicles are demonstrated in Figure 9b. It can be found that the host vehicle can maintain a certain frontal clearance during the simulation. However, as the rear clearance is ignored, a rear-end collision occurred at the back of the host vehicle. The simulation results indicate that it is not sufficient to only consider the frontal clearance of the host vehicle.

As comparison with the scenario without the proposed algorithm, 2 scenarios are evaluated with different friction coefficients. In the 1st scenario, the friction coefficient is high (0.9) and in the 2nd scenario, low (0.5). Moreover, in these scenarios, the mass and inertia of the host vehicle are increased by 10%, which is used to evaluate the robust performance of the proposed algorithm to parameter uncertainties. The speeds and clearances of the vehicles in the high and low friction coefficient scenarios are plotted in Figure 10 and Figure 11, respectively. These figures demonstrate that the clearances among these vehicles are positive along the simulation. At the end of simulation, the following vehicle can follow the host vehicle at the same speed. The path tracking performances of the proposed algorithm on different friction coefficients are further plotted in Figure 12, which indicates that both of the tracking errors in these scenarios are small. The above discussion indicates that, with the proposed algorithm, the front and rear clearances of the host vehicle can be maintained to avoid rear-end collision caused by a following vehicle with different road conditions and parameter uncertainties.

5.3. Simulation on a general curved road with 2 frontal vehicles

In this simulation, a general curved road is considered to further verify the effectiveness of the proposed algorithm. Moreover, 2 accelerating frontal vehicles are considered in the simulation. The initial longitudinal speeds and clearances of these vehicles are shown in Figure 13a. The following vehicle is controlled by a driver without any driver assistant system. The path of the considered curved road is shown in Figure 13b. Due to attention diversion,

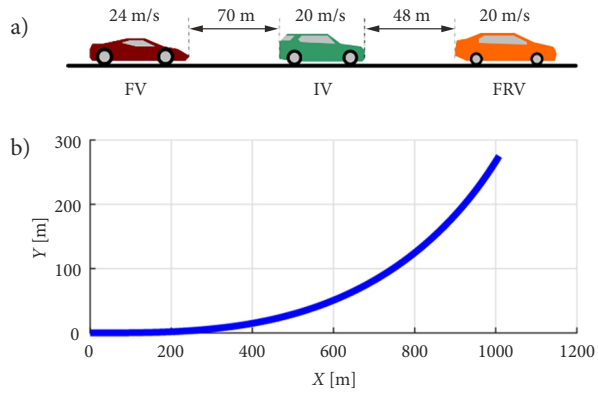

Figure 8. Initial motion states and road path (source: created by the authors): a – initial speeds and clearances; b – path; FV – following vehicle; IV – intelligent vehicle; FRV – frontal vehicle

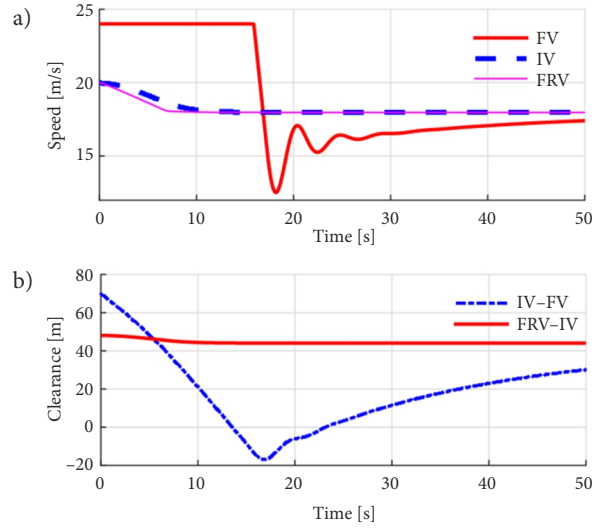

Figure 9. Vehicle speeds and clearances between vehicles (source: created by the authors): a – speeds of vehicles; b – clearances between vehicles; FV – following vehicle; IV – intelligent vehicle; FRV – frontal vehicle

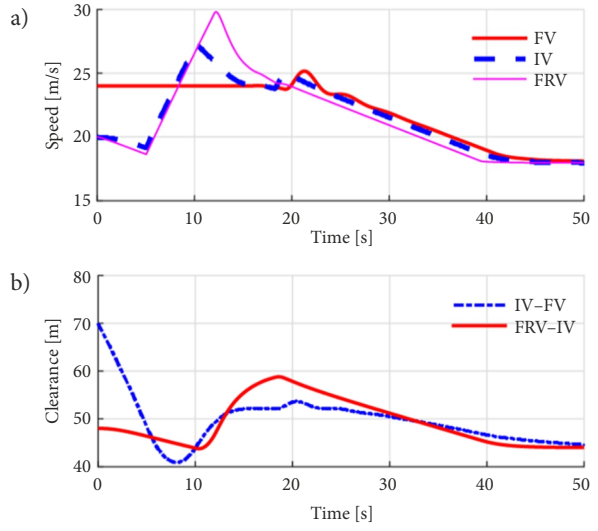

Figure 10. Speeds and clearances of vehicles considering rear-end collision escape with a high friction coefficient (source: created by the authors): a – speeds of vehicles; b – clearances between vehicles; FV – following vehicle; IV – intelligent vehicle; FRV – frontal vehicle

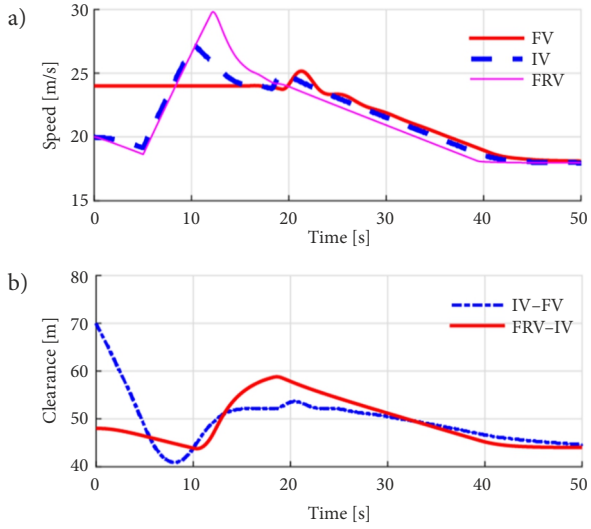

Figure 11. Speeds and clearances of vehicles considering rear-end collision escape with a low friction coefficient (source: created by the authors): a – speeds of vehicles; b – clearances between vehicles; FV – following vehicle; IV – intelligent vehicle; FRV – frontal vehicle

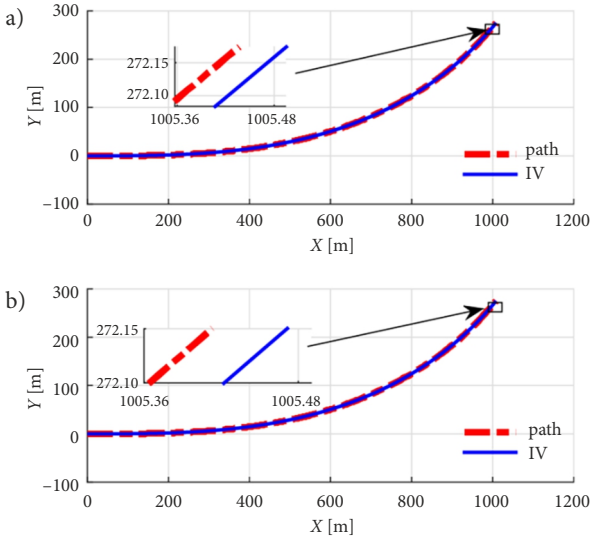

Figure 12. Path tracking performances of vehicles considering rear-end collision escape with different friction coefficients (source: created by the authors): a – high friction coefficient; b – low friction coefficient; IV – intelligent vehicle

the driver of the following vehicle does not brake the vehicle in the beginning. Without considering rear-end collision escape, the speeds and clearances of these vehicles are shown in Figure 14.

It can be seen from Figure 14b that the minimum clearance is lower than zero, which means a rear-end collision occurred due to the wrong manoeuvre of the driver of the following vehicle. Similar to the previous simulations, this simulation also indicates that a driver with attention diversion may cause a rear-end collision on the roadway. It is essential to consider such a dangerous condition for intelligent vehicles.

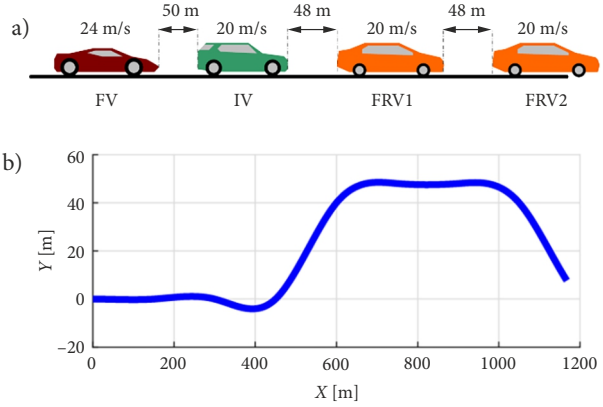

Figure 13. Initial motion states and path (source: created by the authors): a – initial speeds and clearances; b – path; FV – following vehicle; IV – intelligent vehicle; FRV – frontal vehicle

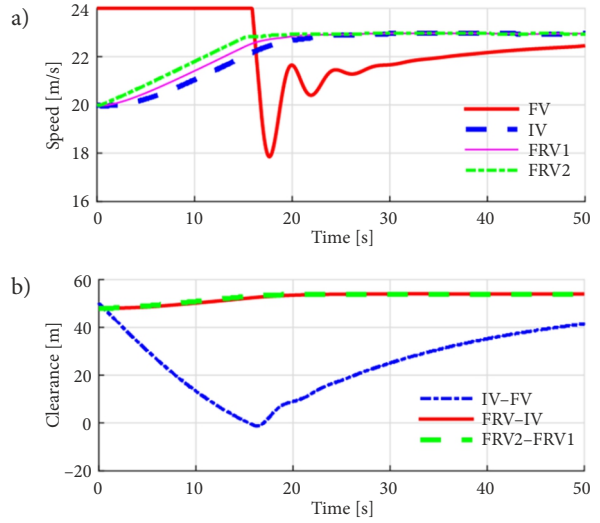

Figure 14. Speeds and clearance of vehicles without considering rear-end collision escape (source: created by the authors): a – speeds of vehicles; b – clearances between vehicles; FV – following vehicle; IV – intelligent vehicle; FRV – frontal vehicle

Using the proposed algorithm, the speeds of these vehicles are shown in Figure 15a. The clearances of these vehicles are shown in Figure 15b. The path tracking performance of the intelligent vehicle is illustrated in Figure 16 with different scopes of view. The drive torque and steering angle of the intelligent vehicle are plotted in Figure 17.

Figure 15b indicates that the actual clearance during simulation is higher than zero, which means there is no rear-end collision during the simulation. Comparing Figures 15b and 14b, it can be found that the proposed algorithm is effective in preventing rear-end collisions caused by a following vehicle. Controlled by the proposed algorithm, the intelligent vehicle can maintain a safe front and rear clearance and avoid potential rear-end collisions. Figure 16 shows that the intelligent vehicle can follow the road path with small tracking error, which demonstrates a good lane keeping performance of the proposed algorithm.

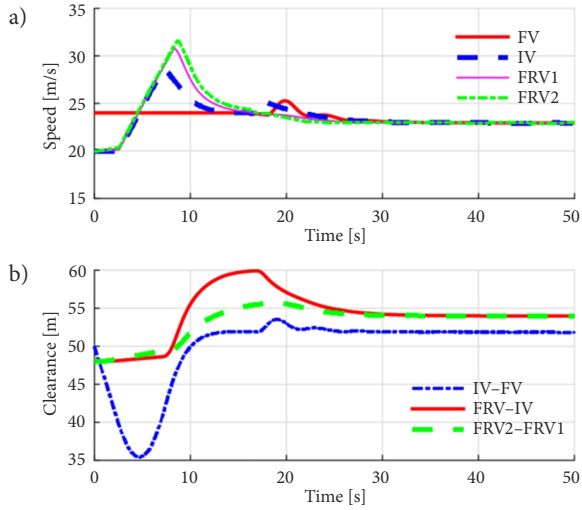

Figure 15. Speeds and clearance of vehicles considering rear-end collision escape (source: created by the authors): a – speeds of vehicles; b – clearances between vehicles; FV – following vehicle; IV – intelligent vehicle; FRV – frontal vehicle

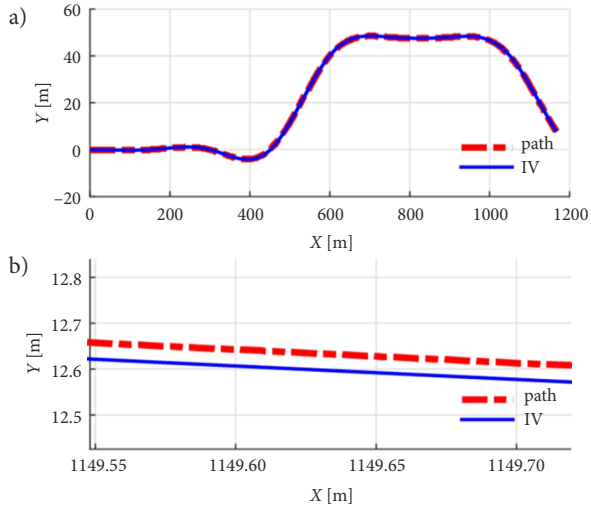

Figure 16. Path tracking of the intelligent vehicle (source: created by the authors): a – global view; b – local view; IV – intelligent vehicle

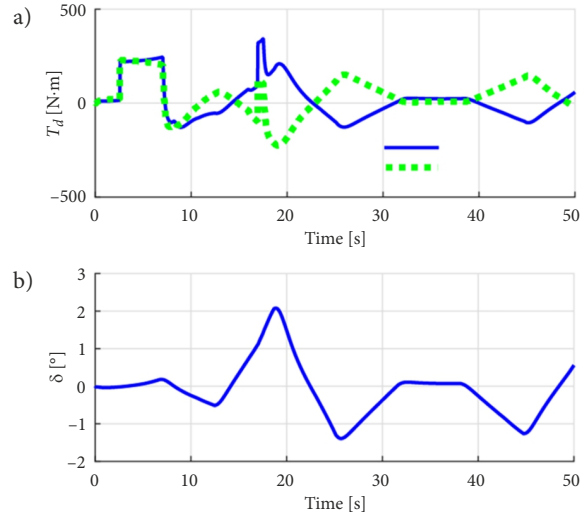

Figure 17. Control inputs (source: created by the authors): a – drive torque; b – steering angle

This simulation demonstrates that the proposed algorithm can handle the vehicle longitudinal and lateral dynamics simultaneously. Both of the requirements of rear-end collision escape and vehicle following can be guaranteed on a curved road. Thus, the proposed algorithm can be employed for a wide-ranging field to improve traffic safety.

Conclusions

In this paper, the algorithm for rear-end collision escape on a common road is proposed.

Compared with previous rear-end collision avoidance algorithms, the uniqueness of the proposed algorithm is that, the potential rear-end accident of the back of the host vehicle can be avoided. When the algorithm detects that the host vehicle may be collided by a following vehicle, the algorithm will control the host vehicle to accelerate to maintain a safe clearance with the following vehicle and send safe trajectories to frontal vehicles. Moreover, the performance of path tracking can also be guaranteed based on the proposed algorithm.

By contrast, most of the previous relevant studies only considered the reduction of frontal rear-end collisions on straight roads. The previous algorithms will not start when a following vehicle is about to collide with the host vehicle, which is not sufficient for actual application.

Based on the proposed algorithm, in a traffic system, the rear-end collision accidents caused by following vehicles can be reduced. Thus, a reduction of rear-end collisions and fatal traffic accidents can be expected with the application of this algorithm.

Funding

This work was supported by: the National Natural Science Foundation of China (Grants No U1664258, 51575103), the National Key R&D Program in China (Grants No 2016YFB0100906, 2016YFD0700905), the Foundation of State Key Laboratory of Automotive Simulation and Control (Grant No 20160112), the Scientific Research Foundation of Graduate School of Southeast University and Southeast University Excellent Doctor Degree Thesis Training Fund (Grant No YBJJ1703).

Disclosure statement

All authors have no conflict of interest.

References

Andersen, G. J.; Sauer, C. W. 2007. Optical information for car following: the driving by visual angle (DVA) model, *Human Factors: the Journal of the Human Factors and Ergonomics Society* 49(5): 878–896. https://doi.org/10.1518/001872007X230235

Benedetto, F.; Calvi, A.; D'Amico, F.; Giunta, G. 2015. Applying telecommunications methodology to road safety for rear-end collision avoidance, *Transportation Research Part C: Emerging Technologies* 50: 150–159. https://doi.org/10.1016/j.trc.2014.07.008

Birgin, E. G.; Mario Martínez, J. 2002. Large-scale active-set box-constrained optimization method with spectral projected gradients, *Computational Optimization and Applications* 23(1): 101–125. https://doi.org/10.1023/A:1019928808826

Camacho, E. F.; Bordons, C. 2007. *Model Predictive Control*. Springer. 405 p. https://doi.org/10.1007/978-0-85729-398-5

Chen, C.; Liu, H.; Xiang, H.; Li, M.; Pei, Q.; Wang, S. 2016. A rear-end collision avoidance scheme for intelligent transportation system, *MATEC Web of Conferences* 81: 02001. https://doi.org/10.1051/matecconf/20168102001

Deng, T. 2000. *Research on Feedback Correction and Greenhouse Control Using Predictive Control*. Tongji University, China. (in Chinese).

Eskandarian, A. 2012. *Handbook of Intelligent Vehicles*. Springer. 1599 p. https://doi.org/10.1007/978-0-85729-085-4

Fildes, B. 2012. Safety benefits of automatic emergency braking systems in France, *SAE Technical Paper* 2012-01-0273. https://doi.org/10.4271/2012-01-0273

Fildes, B.; Keall, M.; Bos, N.; Lie, A.; Page, Y.; Pastor, C.; Pennisi, L.; Rizzi, M.; Thomas, P.; Tingvall, C. 2015. Effectiveness of low speed autonomous emergency braking in real-world rear-end crashes, *Accident Analysis & Prevention* 81: 24–29. https://doi.org/10.1016/j.aap.2015.03.029

Hoogendoorn, R. G.; Tamminga, G., Hoogendoorn, S. P.; Daamen, W. 2010. Longitudinal driving behavior under adverse weather conditions: adaptation effects, model performance and freeway capacity in case of fog, in *13th International IEEE Conference on Intelligent Transportation Systems*, 19–22 September 2010, Funchal, Portugal, 450–455. https://doi.org/10.1109/ITSC.2010.5625046

Kavitha, K. V. N.; Bagubali, A.; Shalini, L. 2009. V2V wireless communication protocol for rear-end collision avoidance on highways with stringent propagation delay, in *2009 International Conference on Advances in Recent Technologies in Communication and Computing*, 27–28 October 2009, Kottayam, India, 661–663. https://doi.org/10.1109/ARTCom.2009.173

Kim, D.-J.; Park, K.-H.; Bien, Z. 2007. Hierarchical longitudinal controller for rear-end collision avoidance, *IEEE Transactions on Industrial Electronics* 54(2): 805–817. https://doi.org/10.1109/TIE.2007.891660

Li, L.; Lu G.; Wang, Y.; Tian, D. 2014. A rear-end collision avoidance system of connected vehicles, in *17th International IEEE Conference on Intelligent Transportation Systems* (*ITSC*), 8–11 October 2014, Qingdao, China, 63–68. https://doi.org/10.1109/ITSC.2014.6957667

Li, X.; Luo, X.; He, M.; Chen, S. 2018. An improved car-following model considering the influence of space gap to the response, *Physica A: Statistical Mechanics and its Applications* 509: 536–545. https://doi.org/10.1016/j.physa.2018.06.069

Li, Y.; Zhang, L.; Song. Y. 2016. A vehicular collision warning algorithm based on the time-to-collision estimation under connected environment, in *2016 14th International Conference on Control, Automation, Robotics and Vision* (*ICARCV*), 13–15 November 2016, Phuket, Thailand, 1–4. https://doi.org/10.1109/ICARCV.2016.7838789

Lv, H.; Xu, P.; Chen, H.; Zhou, B.; Ren, T.; Chen, Y. 2016. A novel rear-end collision warning algorithm in VANET, in *2016 8th IEEE International Conference on Communication Software and Networks* (*ICCSN*), 4–6 June 2016, Beijing, China, 539–542. https://doi.org/10.1109/ICCSN.2016.7586581

Meng, F.; Gray, R.; Ho, C.; Ahtamad, M.; Spence, C. 2015. Dynamic vibrotactile signals for forward collision avoidance warning systems, *Human Factors: the Journal of the Human Factors and Ergonomics Society* 57(2): 329–346. https://doi.org/10.1177/0018720814542651

Nekovee, M.; Bie, J. 2013. Rear-end collision: causes and avoidance techniques, in R. Naja (Ed.). *Wireless Vehicular Networks for Car Collision Avoidance*, 99–119. https://doi.org/10.1007/978-1-4419-9563-6_4

Petrovai, A.; Danescu, R.-G.; Negru, M.; Vancea, C.-C.; Nedevschi, S. 2016. A stereovision based rear-end collision warning system on mobile devices, in *2016 IEEE 12th International Conference on Intelligent Computer Communication and Processing* (*ICCP*), 8–10 September 2016, Cluj-Napoca, Romania, 285–292. https://doi.org/10.1109/ICCP.2016.7737161

Rakha, H.; Pasumarthy, P.; Adjerid, S. 2009. A simplified behavioral vehicle longitudinal motion model, *Transportation Letters: the International Journal of Transportation Research* 1(2): 95–110. https://doi.org/10.3328/TL.2009.01.02.95-110

Rizzi, M.; Kullgren, A.; Tingvall, C. 2014. Injury crash reduction of low-speed autonomous emergency braking (AEB) on passenger cars, in *2014 IRCOBI Conference Proceedings*, 10–12 September 2014, Berlin, Germany, 656–665. Available from Internet: http://www.ircobi.org/wordpress/downloads/irc14/pdf_files/73.pdf

Shah, J.; Best, M.; Benmimoun, A.; Ayat, M. L. 2015. Autonomous rear-end collision avoidance using an electric power steering system, *Proceedings of the Institution of Mechanical Engineers, Part D: Journal of Automobile Engineering* 229(12): 1638–1655. https://doi.org/10.1177/0954407014567517

Wächter, A.; Biegler, L. T. 2006. On the implementation of an interior-point filter line-search algorithm for large-scale nonlinear programming, *Mathematical Programming* 106(1): 25–57. https://doi.org/10.1007/s10107-004-0559-y

Wu, Y.; Abdel-Aty, M.; Park, J. 2017. Developing a rear-end crash risk algorithm under fog conditions using real-time data, in *2017 5th IEEE International Conference on Models and Technologies for Intelligent Transportation Systems* (*MT-ITS*), 26–28 June 2017, Naples, Italy, 568–573. https://doi.org/10.1109/MTITS.2017.8005736

Yang, L.; Yang, J, H.; Feron, E.; Kulkarni, V. 2003. Development of a performance-based approach for a rear-end collision warning and avoidance system for automobiles, in *IEEE IV2003 Intelligent Vehicles Symposium. Proceedings*, 9–11 June 2003, Columbus, OH, US, 316–321. https://doi.org/10.1109/IVS.2003.1212929

Yin, G.-D.; Chen, N.; Wang, J.-X.; Wu, L.-Y. 2011. A study on μ-synthesis control for four-wheel steering system to enhance vehicle lateral stability, *Journal of Dynamic Systems, Measurement, and Control* 133(1): 011002. https://doi.org/10.1115/1.4002707

Zhai, Y.; Nounou, M.; Nounou, H.; Al-Hamidi, Y. 2010. Model predictive control of a 3-DOF helicopter system using successive linearization, *International Journal of Engineering, Science and Technology* 2(10): 9–19. https://doi.org/10.4314/ijest.v2i10.64008